Liu, W., Duan, R., Chen, C., Lin, C.-H., and Chen, Q. "Inverse design of the thermal environment in and airliner cabin by use of the CFD-based adjoint method," Accepted by *Energy and Buildings*.

Inverse design of the thermal environment in an airliner cabin by use of the CFD-based adjoint method

Wei Liu[1,2], Ran Duan[2], Chun Chen[1], Chao-Hsin Lin[3], Qingyan Chen[1,2*]

[1]School of Mechanical Engineering, Purdue University, West Lafayette, IN 47907, USA
[2]Tianjin Key Laboratory of Indoor Air Environmental Quality Control, School of Environmental Science and Engineering, Tianjin University, Tianjin 300072, China
[3]Environmental Control Systems, Boeing Commercial Airplanes, Everett, WA 98203, USA

[*]Corresponding author:

Email:yanchen@purdue.edu
Address: School of Mechanical Engineering, Purdue University, 585 Purdue Mall, West Lafayette, IN 47907-2088
Phone: (765) 496-7562, FAX: (765) 494-0539

Highlights

- The adjoint method was applied to inverse design of thermal environment
- The design method is innovative for thermal environment
- The design used the mixed and displacement ventilation systems as examples
- The design process can identify the optimal variables in less than 10 design cycles

Abstract

The current thermal environments in airliner cabins may not provide satisfactory comfort levels, and the design of these environments should be improved. This study aimed to design a desirable thermal environment for a single-aisle airliner cabin and used the CFD-based adjoint method to find the optimal design variables of air supply locations, size, and parameters. The design variables are used as the boundary conditions for solving the Navier-stokes equations. By setting the occupant region as the design domain with a minimal predicted mean vote for thermal comfort, this study aimed to determine the corresponding air supply conditions for mixing and displacement ventilation systems under summer and winter conditions. The results show that it is possible to find the optimal air supply conditions in fewer than 10 design cycles if the initial conditions for design variables are provided within a reasonable range. This design method has a high computing efficiency as it takes one hour for a design cycle using a 16-core cluster. In addition, the results show that a displacement ventilation system provides a better thermal comfort level than a mixing ventilation system.

Keywords: Airliner cabin; Adjoint method; Thermal comfort; Predicted mean vote

Nomenclature

Symbol definition

D	rate of strain tensor

	f	clothing area factor
	$\mathbf{g}$	gravity vector
	O	objective function
	h	convective heat transfer coefficient
	I	thermal resistance of clothing
	l_{in}	inlet size
	L	augmented objective function
	M	metabolic activity
	p	air pressure
	p_w	partial water vapor pressure
	PMV	predicted mean vote
	PMV_c	predicted mean vote for airliner cabin
	$\mathbf{N}$	Navier-Stokes equations in vector form
	N_1	continuity equation
	N_2, N_3, N_4	momentum equations
	N_5	energy equation
	t	clothing temperature
	T	air temperature
	T_{op}	operating temperature
	T_r	mean radiant temperature
	$\mathbf{U}$	air velocity vector
	W	external work
	x, y, z	index of coordinates

Subscripts

a	adjoint parameter
in	inlet
x	component in x direction
y	component in y direction
z	component in z direction

Greek symbols

γ	thermal expansion coefficient
δ	variation
Θ	computational domain
κ	effective conductivity
λ, ψ, ϕ	positive constants
ν	effective viscosity
$\boldsymbol{\xi}$	design variable vector
Ω	design domain

1. Introduction

An aircraft cabin is a space with high occupant density, and passengers typically spend between one and 15 hours on board. Environmental control systems are used to provide a

comfortable and safe environment for the passengers. The operating power of an environmental control system in a 400-passenger airliner can be as high as 350 kW, which is about 75% of all non-propulsive energy consumption on board (Majeed and Eng, 2010). Even with such high energy consumption, the cabin environment is often unsatisfactory. Haghighat et al. (1999) investigated the thermal environment on 43 commercial flights. Their study found that the air temperature was often below the recommended range of 23 to 26 ^{o}C, and the relative humidity was always too low in comparison with the recommended minimum level of 30% in ASHRAE Standard 55–92 (1992). Park et al. (2011) showed that 25% of passengers were not satisfied with the thermal environment, as the upper body was too warm or the lower body was too cold. Therefore, the design of the cabin environment needs to be further improved to ensure that it is comfortable and healthy for the flying public and crew members.

The conventional design process uses "trial and error" to evaluate the cabin environment and iteratively adjust design parameters such as air supply airflow rate, temperature, humidity, and other thermo-fluid boundary conditions. Evaluation of the cabin environment requires information about air velocity, air temperature, contaminant concentrations, etc., which can be obtained by use of analytical and empirical models, experimental measurements, and computer simulations (Chen, 2009). With the rapid development of computer technology in recent years, simulation of the information by means of computational fluid dynamics (CFD) has become popular for buildings (Chen, 2009) and airliner cabins (Liu et al., 2012). Although CFD is a valuable tool, it can be computationally demanding. The use of CFD in the conventional "trial-and-error" design process would involve a large number of simulations and would therefore entail days or even weeks of computing for completion of a design. Furthermore, it is unlikely that the conventional procedure would be capable of determining the design variables that best meet the desired objective (Jameson, 1988).

In the design of a cabin environment, there are several promising approaches to speeding up the process and identifying the optimal design. These include the CFD-based genetic algorithm (GA) method, proper orthogonal decomposition (POD) analysis, and CFD-based adjoint method (Liu et al. 2015). GA was developed to simulate natural evolution in searching for optimal solutions (Holland, 1975). The CFD-based GA method has been applied to the optimization and inverse design of an enclosed environment (Zhou and Haghighat, 2009a, 2009b; Xue et al., 2013; Zhai et al., 2014). This method is superior for finding the globally optimal conditions and can effectively reduce the total number of iterations needed to reach one or more optimal solutions, as compared with the traditional "trial-and-error" process (Bosworth, 1972). However, the combination of CFD and GA still requires a prohibitively large number of CFD simulations. In order to reduce the simulation effort, POD analysis uses 10 or fewer CFD simulations to describe the characteristics of the indoor air distribution and then uses an offline-online procedure to provide a very quick cause-effect mapping between the design variables and design objective (Rozza et al., 2008; Haasdonk and Ohlberger, 2011). POD analysis has been successfully applied in the optimization and inverse design of an enclosed environment (Sempey et al., 2008; Li et al., 2012, 2013). However, because of the nonlinear nature of the indoor environment, the method may not be accurate. The adjoint method computes the derivative of the design objective with respect to design variables in order to determine the search direction for optimization, and thus the method may identify local optima (Gunzburger et al., 1989, 1991, 1992, 1999). The CFD-based adjoint method requires a lower computing load than the CFD-based GA method. This difference occurs because the adjoint method can determine the sensitivity of the objective function to variations in design variables, and the computing effort

remains the same regardless of the number of design variables (Jameson, 1995). Furthermore, a CFD-based adjoint method can be more accurate than POD analysis, as the adjoint method solves the Navier-stokes equations directly with suitable turbulence models by using the actual thermo-fluid boundary conditions. However, the adjoint method may find local optima and is often mathematically complex, so it has not been widely used for indoor environmental design. Our previous studies (Liu and Chen, 2014; Liu et al., 2015) have validated this method for determining thermo-fluid boundary conditions for desirable air velocity and temperature distribution in a two-dimensional cavity by means of inverse design. The results demonstrated that the adjoint method is accurate and stable, although it may lead to locally optimal solutions.

The present study used the adjoint method for inverse design of the complex thermal environment of an airliner cabin. For a complicated case such as this, it can be very challenging to define a desirable design objective, obtain accurate results, and reduce computing costs. This paper describes our effort in these areas.

2. Research Method

This section describes the process of defining a desirable design objective, determining the design parameters, and using the CFD-based method in the inverse design of the thermal environment in an airliner cabin.

2.1 Design objective

In an enclosed environment such as a building, the desired thermal comfort level can be determined by means of the predicted mean vote (PMV) index (Fanger 1970). Because an air cabin environment has a lower pressure, which will decrease human body heat loss through convection and increase that through evaporation (Cui et al., 2014), direct use of PMV may not be appropriate. This study used a modified predicted mean vote for air cabins (PMV_c) developed by Cui et al. (2015) that accounts for low pressure in a cruising aircraft cabin. PMV_c can be determined from PMV as shown in Eqs. (1) and (2) for the summer and winter seasons, respectively:

$$PMV_c(\text{summer}) = -0.0758PMV^2 + 0.6757PMV - 0.1262 \quad (1)$$

$$PMV_c(\text{winter}) = -0.0696PMV^2 + 0.6906PMV - 0.1369 \quad (2)$$

As with the PMV scale, the PMV_c scale ranges from -3 (cold) to 0 (neutral) to 3 (hot). The value of PMV can be calculated by:

$$\begin{aligned}\text{PMV}=&(0.303e^{-0.036M}+0.028)\{M-W-3.05\times10^{-3}\times[5733-6.99(M-W)-p_w]\\&-0.42\times[(M-W)-58.15]-1.7\times10^{-5}M(5867-p)-0.0014M(34-T)\\&-3.96\times10^{-8}f\times[(t+273)^4-(T_r+273)^4]-fh(t-T)\}\end{aligned} \quad (3)$$

where

$$t = 35.7 - 0.028(M-W) - I\{3.96\times10^{-8}f\times[(t+273)^4-(T_r+273)^4]+fh(t-T)\} \quad (4)$$

$$h = \begin{cases} 2.38(t-T)^{0.25} \text{ if } 2.38(t-T)^{0.25} > 12.1\sqrt{|\mathbf{U}|} \\ 12.1\sqrt{|\mathbf{U}|} \text{ if } 2.38(t-T)^{0.25} < 12.1\sqrt{|\mathbf{U}|} \end{cases} \quad (5)$$

$$f = \begin{cases} 1.00 + 1.290I \quad \text{for } I \le 0.078 m^2 {}^\circ C / W \\ 1.05 + 0.645I \quad \text{for } I > 0.078 m^2 {}^\circ C / W \end{cases} \quad (6)$$

In these equations, W (W) is the external work accomplished, M (W/m^2) the metabolic activity, I (clo) the thermal resistance of the passengers' clothing, T (°C) the air temperature, T_r (°C) the mean radiant temperature, $\mathbf{U}$ (m/s) the air velocity, and p_w (Pa) the relative humidity or partial water vapor pressure.

The design objective of this study was to achieve the most thermally comfortable cabin environment, where PMV_c should approach zero. Thus, the corresponding objective function was constructed as:

$$O(\boldsymbol{\xi}) = \int_{\Omega} (PMV_c)^2 d\Omega \Big/ \int_{\Omega} d\Omega \quad (7)$$

where Ω is the design domain, which is normally the area around the passengers, and $\boldsymbol{\xi}$ is a vector that denotes a series of design variables.

2.2 Design parameters

In an aircraft cabin, many of the parameters used to calculate PMV_c are known. For example, this study set the metabolic activity level to 75 W for passengers in a relaxed mood (in-flight) and the thermal resistance of the passengers' clothing (clo) to 0.57 clo for summer and 1.01 clo for winter (ASHRAE Handbook, 2005). The external work accomplished was assumed to be 0 W. Considering the low relative humidity and low pressure situation in an aircraft cabin (Nagda and Hodgson, 2001; Park et al., 2011), the partial water vapor pressure (p_w) of ambient air was set to 221.8 Pa, which corresponds to an average relative humidity of 13% inside a cruising aircraft. For simplicity, this study assumed the mean radiation temperature to be the same as the air temperature in the cabin. Then the PMV becomes a function only of air temperature and velocity.

The air temperature and velocity fields in an aircraft cabin are determined primarily by design variables such as the geometry of the cabin interior furnishings, internal thermal loads, air supply velocity and temperature from the diffusers and gaspers, inlet size and location, etc. For the purpose of demonstrating the adjoint method, this study set only the air supply location, size, velocity, and temperature from the diffusers as the design variables. It should be noted that the computing time needed by the adjoint method does not depend on the number of variables.

When PMV_c is used to evaluate the thermal environment in the air cabin, with the above assumptions, we have the following variables and equations for inverse design of the air cabin environment:

- State variables: air velocity $\mathbf{U}$ (vector), air pressure p, and air temperature T;
- Design variables $\boldsymbol{\xi}$: inlet location y_{in}, inlet size l_{in}, inlet air velocity $\mathbf{U}_{\text{in}}$ (vector), and inlet air temperature T_{in}. $\boldsymbol{\xi} = (y_{in}, l_{in}, \mathbf{U}_{\text{in}}, T_{in})$;

- State equations for the airflow in the domain, which are Navier-stokes (NS) equations denoted by $\mathbf{N} = (N_1, N_2, N_3, N_4, N_5)$:

$$N_1 = -\nabla \cdot \mathbf{U} = 0 \tag{8}$$

$$(N_2, N_3, N_4)^T = (\mathbf{U} \cdot \nabla)\mathbf{U} + \nabla p - \nabla \cdot (2\nu D(\mathbf{U})) - \gamma \mathbf{g}(T - T_{op}) = 0 \tag{9}$$

$$N_5 = \nabla \cdot (\mathbf{U}T) - \nabla \cdot (\kappa \nabla T) = 0 \tag{10}$$

This investigation applied the re-normalization group (RNG) k-ε model (Yakhot and Orszag, 1986), which is widely used for indoor airflow modeling (Zhang et al., 2007), to simulate turbulence in the state equations. The Boussinesq approximation (Boussinesq, 1903) was applied to simulate the buoyancy effect, while the air density was assumed to be constant. The design goal was to minimize the objective function with state variables subjected to the state equations.

2.3 Design method

This study applied the CFD-based adjoint method, an optimization process which is used to find the design variables that minimize the objective function. The adjoint method computes the derivative of the objective function with respect to the design variables, so that the method can search for the direction that gradually minimizes the objective function. The curve in Figure 1 can be used to represent the relationship between a design variable and the design objective. The adjoint method first initializes a starting point (ξ, $O(\xi)$). The method then computes the gradient and adjusts the design variable in the direction that minimizes the objective function. This procedure is repeated until the minimum has been found. It is possible, of course, that this method will identify only the local optima. However, a reasonable estimate of the ξ can speed up convergence, and thus local optima can be avoided.

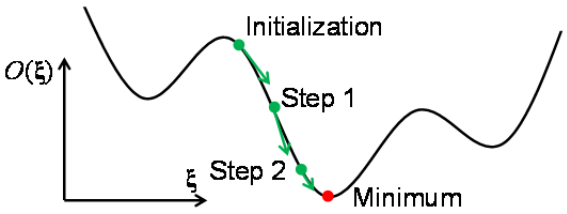

Figure 1. Principle of the adjoint method

With initialized inlet air conditions ξ, this approach computes the state equations in order to locate the starting point (ξ, $O(\xi)$). Next, the gradient of O with respect to ξ needs to be determined in order to find new design variables that will make O smaller. In this study, O is a function of $\mathbf{U}$ and T, but not ξ, and thus the gradient $dO/d\xi$ cannot be directly computed. Since ξ determines $\mathbf{U}$, T, and p and also has an impact on O, the adjoint method introduces a Lagrangian multiplier (p_a, $\mathbf{U}_a$, T_a) to make $dO/d\xi$ computable. Here, p_a, $\mathbf{U}_a$, and T_a are the adjoint velocity, temperature, and pressure, respectively. The Lagrange multiplier is introduced in order to develop an augmented objective function that can be formulated as:

$$L = O + \int_{\Omega} (p_a, \mathbf{U}_a, T_a) \cdot \mathbf{N} d\Theta \tag{11}$$

where Θ represents the computational domain. Since $\mathbf{N} = \mathbf{0}$, the variation of the objective function with respect to the design variable $\boldsymbol{\xi}$ can be expressed as:

$$dO \approx dL = \frac{\partial L}{\partial \boldsymbol{\xi}} \cdot d\boldsymbol{\xi} + \frac{\partial L}{\partial \mathbf{U}} \cdot d\mathbf{U} + \frac{\partial L}{\partial p} dp + \frac{\partial L}{\partial T} dT \tag{12}$$

To find the gradient $dO/d\boldsymbol{\xi}$, the adjoint method sets the last three terms on the right-hand side of Equation (12) to zero. So we have:

$$\frac{\partial L}{\partial \mathbf{U}} \cdot d\mathbf{U} + \frac{\partial L}{\partial p} dp + \frac{\partial L}{\partial T} dT = 0 \tag{13}$$

$$\frac{dO}{d\boldsymbol{\xi}} = \frac{\partial L}{\partial \boldsymbol{\xi}} = \frac{\partial O}{\partial \boldsymbol{\xi}} + \int_{\Omega} (p_a, \mathbf{U}_a, T_a) \frac{\partial \mathbf{N}}{\partial \boldsymbol{\xi}} d\Theta \tag{14}$$

Equation (13) eliminates the contributions of dp, $d\mathbf{U}$, and dT in Equation (12), and the gradient $dO/d\boldsymbol{\xi}$ can then be calculated by Equation (14), which is straightforward. Equation (13) must be fulfilled for any (dp, $d\mathbf{U}$, dT) that is entailed by $d\boldsymbol{\xi}$. The adjoint method sets each of the three partial derivatives in Equation (13) to zero that constructs the adjoint equations. Through a number of derivation steps, the final form of the adjoint equations can be written as:

$$-\nabla \cdot \mathbf{U}_a = 0 \tag{15}$$

$$-\nabla \mathbf{U}_a \cdot \mathbf{U} - (\mathbf{U} \cdot \nabla)\mathbf{U}_a - \nabla \cdot (2\nu D(\mathbf{U}_a)) + \nabla p_a + T_a \nabla T + \mathbf{A} = 0 \tag{16}$$

$$-\mathbf{U} \cdot \nabla T_a - \nabla \cdot (\kappa \nabla T_a) + B = 0 \tag{17}$$

$$\mathbf{A} = \begin{cases} 2 \times \mathrm{PMV} \times \dfrac{\partial \mathrm{PMV}}{\partial \mathbf{U}} & \text{for domain } \Omega \\ \mathbf{0} & \text{for domain } \Theta \setminus \Omega \end{cases} \tag{18}$$

$$B = \begin{cases} 2 \times \mathrm{PMV} \times \dfrac{\partial \mathrm{PMV}}{\partial T} & \text{for domain } \Omega \\ 0 & \text{for domain } \Theta \setminus \Omega \end{cases} \tag{19}$$

The source terms $\mathbf{A}$ and B in the adjoint equations are determined by the results of the state equations. To reduce the calculation load, this study assumed the turbulence to be "frozen" (Dwight et al., 2006; Othmer, 2008), and the turbulent viscosity in the state equations was used for the adjoint diffusion term.

The solutions of the adjoint equations (p_a, $\mathbf{U}_a$, T_a) are then used to compute $dO/d\boldsymbol{\xi}$ in Equation (14). In addition, $\partial \mathbf{N}/\partial \boldsymbol{\xi}$ needs to be evaluated because $\mathbf{N} \neq \mathbf{0}$ numerically. This study calculated this partial derivative by using the finite element method (Schneider and Jimack, 2008). The optimal design variables can thenbe determined by using this gradient along with the

gradient technique for trajectory optimization proposed by Bryson and Ho (1975). The present study used the simple steepest descent algorithm, in which the variation in ξ can be written as:

$$\delta\xi = -\lambda[\frac{\partial O}{\partial \xi} + \int_{\Omega}(p_a, \mathbf{U}_a, T_a)\frac{\partial \mathbf{N}}{\partial \xi} d\Theta]^T \quad (20)$$

$$\xi_{new} = \xi_{old} + \delta\xi \quad (21)$$

where λ represents positive constants. Then the variation in O is always negative, and the value of the objective function will always decrease. With the updated ξ from Eq. (21), the gradient $dO/d\xi$ can be recalculated, creating a design cycle that is repeated until the optimal design variables are identified. The design procedure is analogous to the searching algorithm in Figure 1.

This study implemented the CFD-based adjoint method in OpenFOAM (2007), which is a CFD software program. The solver in OpenFOAM used a semi-implicit method for pressure-linked equations (SIMPLE) algorithm (Patankar and Spalding, 1972) to couple the velocity/adjoint velocity and pressure/adjoint pressure in solving the NS/adjoint equations. The NS/adjoint continuity equations were solved by the generalized geometric-algebraic multi-grid (GAMG) solver (Hackbusch, 1985). In each design cycle, the NS/adjoint equations were calculated with 5000 to 10,000 iterations to ensure convergence. The design convergence criteria were (1) $O < \psi$ in the first design cycle, where ψ is a small positive constant, and (2) $|O_i - O_{i-1}| < \phi$ in the i^{th} design cycle ($i > 1$). The O_{i-1} is the computed objective function in the prior design cycle, and ϕ is also a small positive constant. This study set $\psi = \phi = 0.01$. Since the air supply location and size may vary in the design procedure, this study used the Gambit journal files (GAMBIT CFD Preprocessor, 1998) to automatically regenerate the corresponding mesh. This study did not conduct the grid independence test specifically and the mesh was generated according to the grid independence in an aircraft cabin in our previous study (Liu et al., 2013).

3. Case setup

This investigation conducted an inverse design of the air environment in a single-aisle, fully-occupied air cabin in order to find the optimal air supply conditions for the diffusers. The gaspers were assumed to be closed. To decrease the computing load, this study performed calculations for only half of one row of the cabin, as illustrated in Figure 2. This cabin model has simplifications such as neglecting the under-seat structures, which have very minimal effect on the flow pattern according to the numerical and experimental study of the air distribution in a functional aircraft cabin (Liu et al., 2012; Liu et al., 2013). For such half of one row of the cabin, the generated mesh has 0.7 million unstructured cells. Figure 2(a) shows the conventional ventilation system in an aircraft cabin, which creates mixed ventilation. The inlet and outlet were located in the upper and lower parts of the side wall, respectively. This study also considered displacement ventilation (Figure 2(b)) according to the work of Zhang and Chen (2007). The inlet and outlet of the cabin with displacement ventilation were located in the aisle and the upper part of the side wall, respectively. The design domain Ω was set as the area 0.1 m away from the passengers. To avoid longitudinal flow, this study fixed the U_z as 0 at the inlet in all calculations.

When a ventilation system is designed for an aircraft cabin, the thermo-fluid boundary conditions must be sufficient for removal of the cooling load and compliance with air quality

regulations. ANSI/ASHRAE Standard 161 (2007) requires a minimum ventilation rate of 9.4 L/s per passenger. This standard also specifies that the operative temperature in-flight and on the ground should be between 18.3°C and 23.9°C. In accordance with these standards, and with the assumption that 75% of the total heat dissipated by the passengers is convective (Liu et al., 2013), the inlet air temperature in this study ranged from 13.3°C to 18.9°C at an airflow rate of 9.4 L/s.

Under these constraints, this study initialized five design variables as shown in Table 1. To avoid local optima, the air supply location and temperature were initialized to their median values. For example, the inlet air temperature ranged from 13.3°C to 18.9°C, and T_{in} was initialized to 16.1°C. The inlet location y_{in} was in the range of 0 – y_{mix} (0.409 m) for mixed ventilation and 0 – y_{dis} (0.28 m) for displacement ventilation. For mixed ventilation, the lower bound was 10 cm higher than the passenger's head to avoid the draft effect. For displacement ventilation, the upper bound was the width of the aisle. The initial inlet locations were then set to $y_{mix}/2$ and $y_{dis}/2$. This study set the initial inlet air velocity as $|\mathbf{U}_{in}|$ = 1.5 m/s and its direction as normal to the inlet surface, according to our previous measurements in a functional aircraft cabin (Liu et al., 2012). Since the air flow rate was constrained, the initial inlet size was determined accordingly.

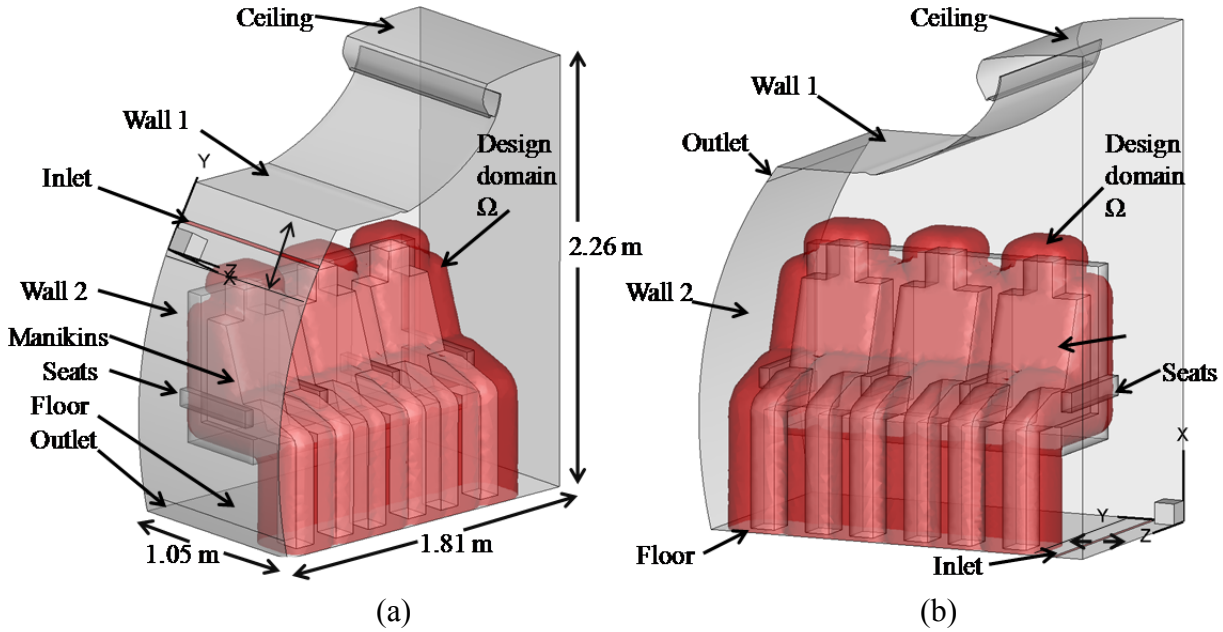

Figure 2. Schematic of the computational domain and design domain for the aircraft cabin: (a) mixed ventilation and (b) displacement ventilation.

Table 1. Ranges and initialized values for the five design variables

Design variable	y_{in} [m]		l_{in} [m]	$U_{in,x}$ [m/s]	$U_{in,y}$ [m/s]	T_{in} [°C]
	Mixed ventilation	Displacement ventilation				
Range	0 – y_{mix}	0 – y_{dis}	N/A	N/A	N/A	13.3 – 18.9
Initialized value	$y_{mix}/2$	$y_{dis}/2$	0.0188	1.5	0	16.1

Table 2 lists the thermal boundary conditions that do not vary during the optimization.

The temperatures of the surfaces shown in Table 2 were obtained from data measured on a flight at cruising altitude by use of an infrared thermometer (Zhang and Chen, 2007).

Table 2. Thermal boundary conditions that were fixed during the optimization

Surface	*T*	Surface	*T*
Wall 1	21°C	Outlet	zero gradient
Wall 2	22°C	Seats	adiabatic
Ceiling	22°C	Floor	23°C
Passengers	30.3°C		

4. Results

This study used the CFD-based adjoint method to find the air supply conditions for the diffusers that would provide the most comfortable thermal environment in the fully-occupied cabin of a single aisle aircraft. To reduce computing time, our study used only half of one row of seats. By using a 16-core cluster with the maximal turbo frequency of 3.3 GHz for each core, it took one hour for a design cycle. Periodic boundary conditions were applied between rows and symmetric boundary conditions in the middle of the aisle.

4.1 Inverse design of the mixed ventilation system

Using the initial air supply conditions in Table 1, Figure 3 shows the changes in the objective function and design variables within 20 design cycles. The objective function and design variables all varied rapidly in the first two design cycles and then became relatively stable in subsequent cycles. The inverse design converged within seven cycles (seven hours' computing time), but the simulation continued until 20 cycles had been completed, as specified. At the end of the optimization process, the objective functions were only 0.16 and 0.06 for summer and winter conditions, respectively. The corresponding averages of the absolute PMV_c in the design domain were 0.40 and 0.24, respectively. The air supply size and velocity exhibited little variation in comparison with the air supply location and temperature. This difference indicates that the thermal comfort level was more sensitive to the air supply location and temperature. Furthermore, the optimal air supply location, size, and velocity were almost the same for both summer and winter, whereas a variation between seasons was observed in the air supply temperature. This variation can be accounted for by the thermal resistance of the passengers' clothing, which changed according to the season.

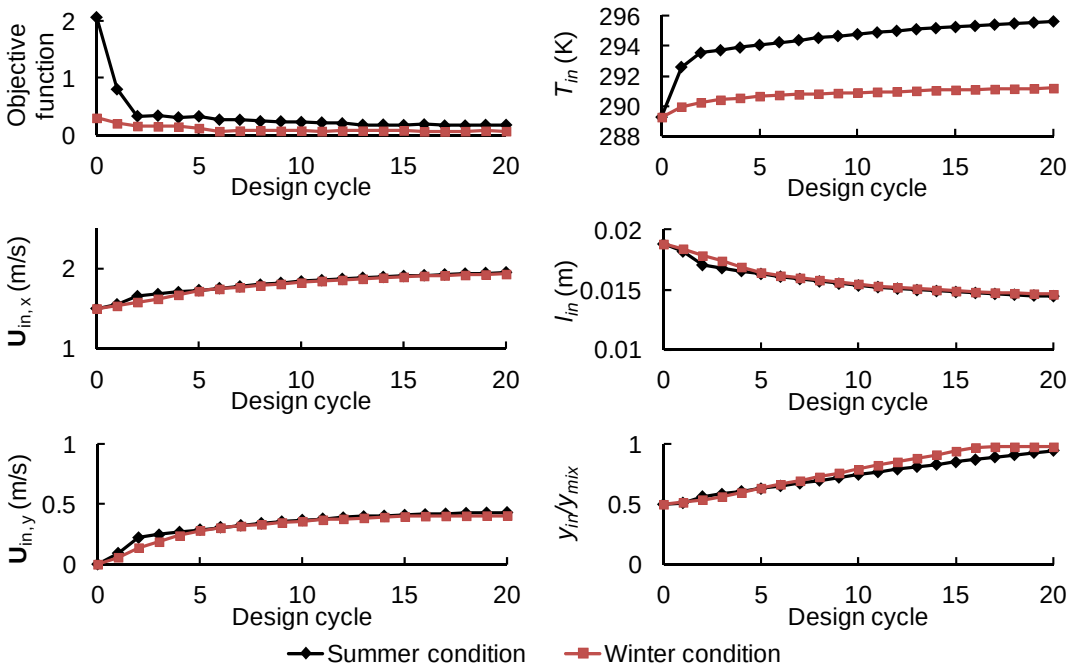

Figure 3. Change in objective function and five design variables versus design cycle for the case of mixed ventilation.

To further demonstrate the sensitivity of the thermal comfort level in the aircraft cabin to the design variables, Figure 4 shows the distribution of air velocity and temperature in the first two design cycles and the last design cycle under summer conditions. The flow and temperature fields changed dramatically during the design process. At the low initial air supply temperature, the air flowed directly toward the passengers at head level, which caused the value of PMV_c to be less than -1, as shown in Figure 4(a). After optimization, the air supply temperature increased, and the air supply location was raised. In the second design cycle (Figure 4(c)), the supplied air did not flow directly toward the passengers at head level and the cabin air temperature increased, which greatly improved the thermal comfort level in the cabin, as shown in Figure 5(c). This change in the flow field was due to the inertial force from the inlet jets is comparable to the buoyancy force from the thermal plumes in the aircraft cabin (Liu et al., 2013). After the 20th design cycle, the inlet location was close to the top of the side wall, and the PMV_c in the design domain was between -0.4 and 0.2, as shown in Figure 5(d). The thermal comfort level in this aircraft cabin was very sensitive to the air supply location and temperature. Figure 5 further shows that the thermal comfort level in this cabin was greatly improved after only two design cycles. Therefore, the CFD-based adjoint method can be very efficient in the inverse design of an enclosed air environment.

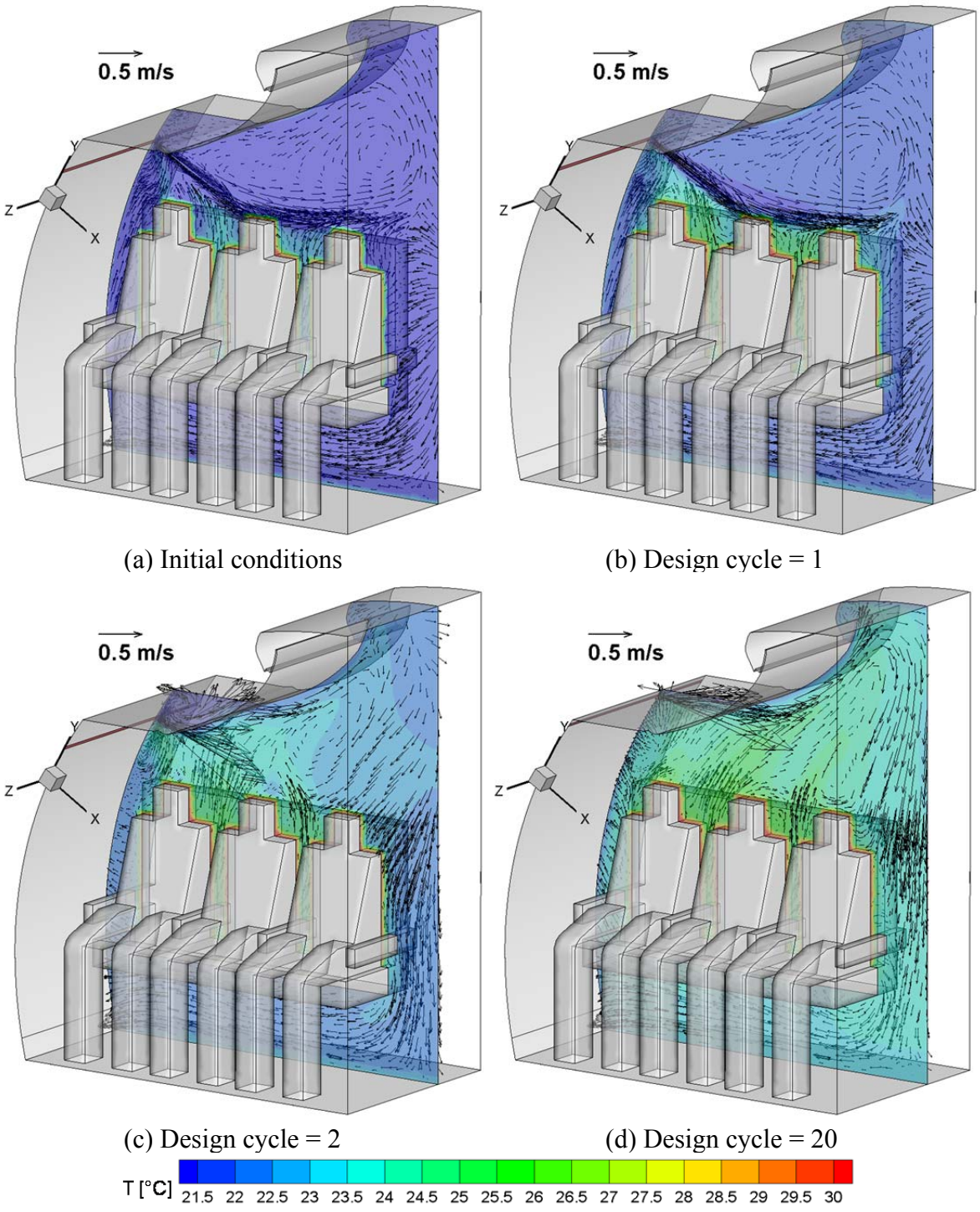

(a) Initial conditions (b) Design cycle = 1

(c) Design cycle = 2 (d) Design cycle = 20

Figure 4. Computed airflow and temperature fields (a) at initial conditions, and after (b) the 1st design cycle, (c) the 2nd design cycle, and (d) the 20th design cycle under summer conditions.

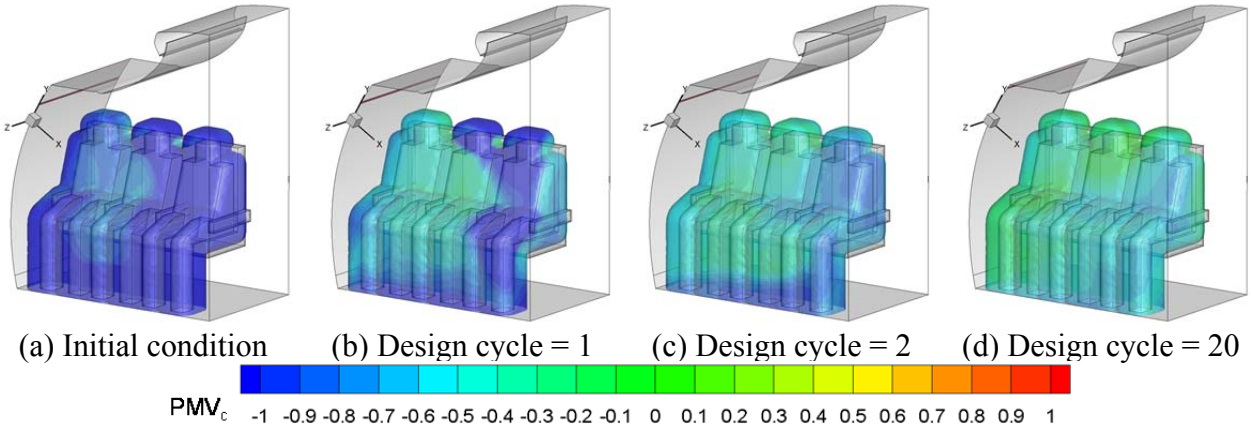

Figure 5. Distribution of PMV_c (a) at initial conditions, and after (b) the 1st design cycle, (c) the 2nd design cycle, and (d) the 20th design cycle under summer conditions.

4.2 Inverse design of the displacement ventilation system

For the displacement ventilation system, this study again followed the inverse design procedure, using the initial air supply conditions in Table 1. Figure 6 shows the change in the objective function and the five design variables within 20 design cycles. As in the case of mixed ventilation, the objective function and design variables varied rapidly in the first five design cycles and then became stable. The optimization converged in the eighth design cycle (eight hours' computing time), in a manner that was similar to but somewhat slower than that of the mixed ventilation case. At the end of the inverse design process, the objective functions were again very small, 0.03 for summer and 0.01 for winter, and led to PMV_c values in the design domain of 0.17 and 0.12, respectively. The thermal comfort level for displacement ventilation was better than that for mixed ventilation. The optimal air supply size and velocity were almost the same in both cases, but the air supply location and temperature were different. The thermal comfort level was more sensitive to the air supply location and temperature. The optimal air supply temperature for displacement ventilation was about 2 K higher than that for mixed ventilation, and this difference has an implication for energy efficiency.

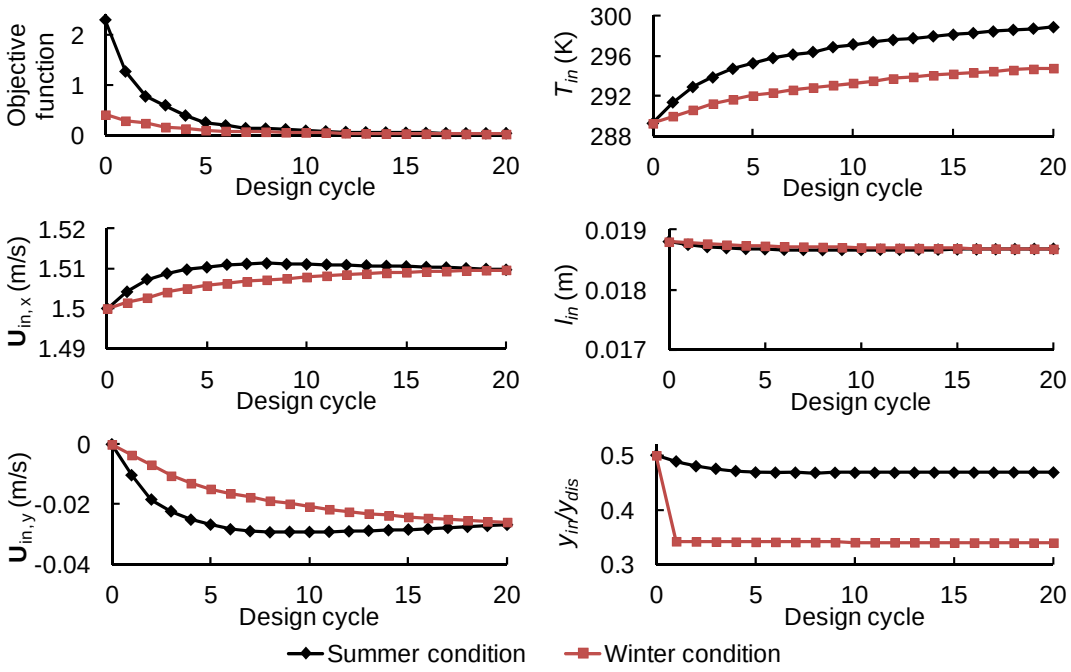

Figure 6. Change in objective function and the five design variables versus design cycle for the case of displacement ventilation.

This study also considered the distribution of PMV_c under summer conditions, as shown in Figure 7. Note that the inverse design process improved the thermal comfort level in this aircraft cabin after five design cycles. After the 20th design cycle (Figure 7(d)), the thermal comfort level was better than that with the mixed ventilation system (Figure 5(d)). The displacement ventilation system can provide a similar thermal comfort level for all three passengers, whereas the mixed ventilation system cannot.

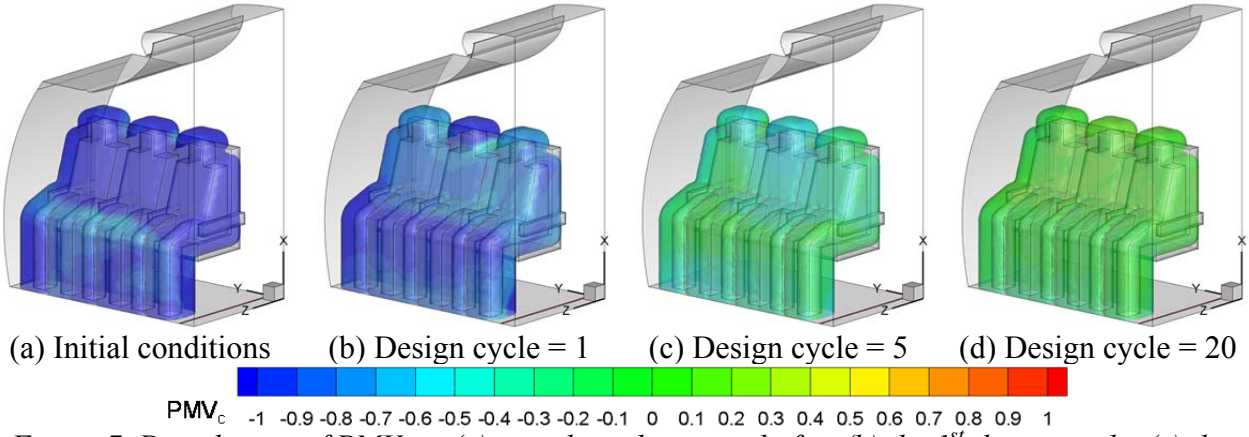

Figure 7. Distribution of PMV_c at (a) initial condition, and after (b) the 1st design cycle, (c) the 5th design cycle, and (d) the 20th design cycle under summer conditions.

5. Discussion

This study conducted an inverse design process that identified the five design variables in a single calculation. The beauty of the adjoint method is that its computing load does not depend on the number of design variables. The optimal PMV_c distribution obtained by this method is

acceptable because the initialized design variables are within a reasonable range. However, the potential for further improvements in the thermal environment of this aircraft cabin is unknown because the method can identify only local optima. Identifying the global optima would require multiple calculations or integration of the method with a gradient-free algorithm. Searching for global optima through a gradient-free algorithm, such as a genetic algorithm, would entail a dramatic increase in the computing cost with an increase in the number of design variables.

This study obtained a converged result within seven to eight design cycles. The difference in convergence speed between the two ventilation systems may have been due to the difference between the initial estimates of the design variables and the optimal values. Furthermore, because this study used the simple steepest descent algorithm, the convergence speed was dependent on λ in Equation (19), which determines the changes in the design variables. This study applied a constant λ to ensure stability. As far as we know, the quasi-Newton method can determine the second derivative of the objective function with respect to the design variables, and therefore the changes in the design variables can be automatically determined in order to speed up the convergence process.

6. Conclusions

This investigation used the CFD-based adjoint method to find the optimal air supply conditions for improving thermal comfort in a single-aisle, fully-occupied air cabin. The PMV_c index was used to evaluate thermal comfort. This study conducted an inverse design of mixed and displacement ventilation systems under summer and winter conditions. The computed results led to the following conclusions:

The CFD-based adjoint method can be used to design a ventilation system that improves thermal comfort in an aircraft cabin. With reasonable estimates of the initial design variables, the optimal variables can be identified in a single calculation.

The optimization process for the displacement ventilation system resulted in a more uniform thermal comfort level than that for the mixed ventilation system. The air temperature with the displacement ventilation system was lower than that with the mixed ventilation system, and this difference has an implication for energy efficiency.

The airflow pattern and thermal comfort level in the cabin were sensitive to the air supply location and temperature. This sensitivity occurred because the inertial force from the inlet jets was comparable to the buoyancy force from the thermal plumes. The optimal air supply temperature differed under summer and winter conditions because of the varying thermal resistance of the passengers' clothing.

Acknowledgement

The research presented in this paper was supported financially by the National Basic Research Program of China (the 973 Program) through Grant No. 2012CB720100 and by the Natural Science Foundation of China through Grant No. 51408413.

References

ASHRAE, 1992. Standard 55-1992, Thermal environmental conditions for human occupancy. ASHRAE, Inc., Atlanta, GA.

513 ASHRAE, 2007. Standard 161-2007, Air quality within commercial aircraft. ASHRAE, Inc.,
514 Atlanta, GA.
515 ASHRAE Handbook., 2005. Thermal Comfort chapter, Fundamentals volume of the ASHRAE
516 Handbook. ASHRAE, Inc., Atlanta, GA.
517 Bosworth, J., Foo, N., Zeigler, B.P., 1972. Comparison of Genetic Algorithms with Conjugate
518 Gradient Methods. NASA (CR-2093). Michigan Press, Washington, D.C.
519 Boussinesq, J., 1903. Th´eorie Analytique de la Chaleur. Gauthier-Villars.
520 Bryson, A.E., Ho, Y.C., 1975. Applied Optimal Control. Hemisphere, Washington, DC.
521 Chen, Q., 2009. Ventilation performance prediction for buildings: A method overview and recent
522 applications. Building and Environment 44(4), 848-858.
523 Cui, W., Ouyang, Q., Zhu, Y., Hu, S. 2014. Prediction model of human thermal sensation under
524 low-air-pressure environment. Proceedings of the 8th International Symposium on Heating,
525 Ventilation and Air Conditioning, 329-336. Springer Berlin Heidelberg.
526 Cui, W., Zhu, Y. 2015. Systematic study on passengers' thermal comfort under low-air-pressure
527 environment in commercial aircraft cabin. Presented in the Annual Meeting of the Center for
528 Cabin Air Reformative Environment (973 project), Chongqing, China.
529 Dwight, R.P., Brezillon, J., 2006. Effect of various approximations of the discrete adjoint on
530 gradient-based optimization. Proceedings of the 44th AIAA Aerospace Sciences Meeting
531 and Exhibit, Reno, NV.
532 Fanger, P.O., 1970. Thermal Comfort, Analysis and Applications in Environmental Engineering,
533 Copenhagen, Danish Technical Press.
534 GAMBIT CFD Preprocessor, 1998. User's Guide. Fluent, Inc., Lebanon, NH.
535 Gunzburger, M., Hou, L., Svobodny, T., 1989. Numerical approximation of an optimal control
536 problem associated with the Navier-Stokes equations. Applied Mathematics 2, 29-31.
537 Gunzburger, M., Hou, L., Svobodny, T., 1991. Analysis and finite element approximation of
538 optimal control problems for the stationary Navier-Stokes equations with distributed and
539 Neumann controls. Mathematics of Computation 57, 123-151.
540 Gunzburger, M., Hou, L., Svobodny, T., 1991. Boundary velocity control of incompressible flow
541 with an application to viscous drag reduction. SIAM Journal on Control and Optimization 30,
542 167-181.
543 Gunzburger, M., 1999. Sensitivities, adjoints and flow optimization. International Journal for
544 Numerical Methods in Fluids 31, 53-78.
545 Haasdonk B, Ohlberger M. 2011. Efficient reduced models and a posteriori error estimation for
546 parametrized dynamical systems by offline/online decomposition. Mathematical and
547 Computer Modelling of Dynamical Systems 17(2), 145-161
548 Hackbusch, W., 1985. Multi-grid Methods and Applications (Vol. 4). Berlin: Springer-Verlag.
549 Haghighat, F., Allard, F., Megri, A. C., Blondeau, P., Shimotakahara, R., 1999. Measurement of
550 thermal comfort and indoor air quality aboard 43 flights on commercial airlines. Indoor and
551 Built Environment 8(1), 58-66.
552 Holland, J., 1975. Adaptation in Natural and Artificial Systems, The University of Michigan
553 Press, Ann Arbor, MI.
554 Jameson, A., 1988. Aerodynamic design via control theory. Journal of Scientific Computing 3,
555 233-260.
556 Jameson, A., 1995. Optimum aerodynamic design using CFD and control theory. AIAA 12th
557 Computational Fluid Dynamics Conference, San Diego, CA, 1995-1729.
558 Li, K., Su, H., Chu, J., Xu, C. 2012. A fast-POD model for simulation and control of indoor

559 thermal environment of buildings. Building and Environment 60, 150-157.
560 Li, K., Xue, W., Xu, C., Su, H. 2013. Optimization of ventilation system operation in office
561 environment using POD model reduction and genetic algorithm. Energy and Buildings 67,
562 34-43.
563 Liu, W., Chen, Q., 2014. Optimal air distribution design in enclosed spaces using an adjoint
564 method. Inverse Problems in Science and Engineering. DOI:
565 10.1080/17415977.2014.933832.
566 Liu, W., Jin, M., Chen, C., Chen, Q. Optimization of air supply location, size, and parameters in
567 enclosed environments using a CFD-based adjoint method. Accepted by Journal of Building
568 Performance Simulation. 2015. DOI: 10.1080/19401493.2015.1006525.
569 Liu, W., Mazumdar, S., Zhang, Z., Poussou, S.B., Liu, J., Lin, C.H., Chen, Q., 2012. State-of-the-
570 art methods for studying air distributions in commercial airliner cabins. Building and
571 Environment 47, 5-12.
572 Liu, W., Wen, J., Chao, J., Yin, W., Shen, C., Lai, D., Lin, C.H., Liu, J., Sun, H., Chen, Q., 2012.
573 Accurate and high-resolution boundary conditions and flow fields in the first-class cabin of
574 an MD-82 commercial airliner. Atmospheric Environment 56, 33-44.
575 Liu, W., Wen, J., Lin, C.H., Liu, J., Long, Z., Chen, Q., 2013. Evaluation of various categories of
576 turbulence models for predicting air distribution in an airliner cabin. Building and
577 Environment 65, 118-131.
578 Majeed, O., Eng, P., 2010. Aircraft environmental control systems. Carleton University Aero
579 Lecture, 4003.
580 Nagda, N., Hodgson, M., 2001. Low relative humidity and aircraft cabin air quality. Indoor
581 Air 11(3), 200-214.
582 OpenFOAM, 2007. The Open Source CFD Toolbox. http://www.opencfd.co.uk/openfoam.html.
583 Othmer, C., 2008. A continuous adjoint formulation for the computation of topological and
584 surface sensitivities of ducted flows. International Journal for Numerical Methods in Fluids
585 58, 861-877.
586 Park, S., Hellwig, R.T., Grün, G., Holm, A., 2011. Local and overall thermal comfort in an
587 aircraft cabin and their interrelations. Building and Environment 46(5), 1056-1064.
588 Patankar, S.V., Spalding, D.B., 1972. A calculation procedure for heat, mass and momentum
589 transfer in three-dimensional parabolic flows. International Journal of Heat and Mass
590 Transfer 15(10), 1787-1806.
591 Rozza, G., Huynh, D., Patera, A., 2008. Reduced basis approximation and a posteriori error
592 estimation for affinely parametrized elliptic coercive partial differential equations. Archives
593 of Computational Methods in Engineering 15(3), 229-275.
594 Sempey, A., Inard, C., Ghiaus, C., Allery, C., 2008. A state space model for real-time control of
595 the temperature in indoor space-principle, calibration and results. International Journal of
596 Ventilation 6(4), 327-336.
597 World Health Organization (WHO), 2009. Chronology of Influenza A (H1N1).
598 Xue, Y., Zhai, Z., Chen, Q., 2013. Inverse prediction and optimization of flow control conditions
599 for confined spaces using a CFD-based genetic algorithm. Building and Environment 64,
600 77-84.
601 Yakhot, V., Orszag, S.A., 1986. Renormalization group analysis of turbulence. Journal of
602 Scientific Computing 1(1), 3-51.
603 Zhai, Z., Xue, Y., and Chen, Q., 2014. Inverse design methods for indoor ventilation systems
604 using CFD-based multi-objective genetic algorithm. Building Simulation 7(6), 661-669.

605 Zhang, T., Chen, Q., 2007. Novel air distribution systems for commercial aircraft cabins.
606 Building and Environment 42(4), 1675-1684.
607 Zhang, Z., Zhang, W., Zhai, Z., Chen, Q., 2007. Evaluation of various turbulence models in
608 predicting airflow and turbulence in enclosed environments by CFD: Part-2: Comparison
609 with experimental data from literature. HVAC&R Research 13(6), 871-886.
610 Zhou, L., Haghighat, F., 2009. Optimization of ventilation system design and operation in office
611 environment, Part I: Methodology. Building and Environment 44(4), 651-656.
612 Zhou, L., Haghighat, F., 2009. Optimization of ventilation systems in office environment, Part II:
613 Results and discussions. Building and Environment 44(4), 657-665.